Advances in research on nickel production through the Caron process

M. Akbar Rhamdhani[1], Jiang Chen[2], Taufiq Hidayat[2], Evgueni Jak[2], Peter Hayes[2]

[1] Faculty of Engineering and Industrial Sciences, Swinburne University of Technology
John St, Hawthorn, Melbourne VIC 3122, Australia
[2] Pyrometallurgy Research Centre, School of Engineering, The University of Queensland
Brisbane, QLD 4072, Australia

Abstract

New environmental and chemical policy regulations require further optimisation of current nickel production processes. This paper outlines recent fundamental research in support of improvements in nickel production process through the Caron Process. The research focuses on two major areas: (i) reduction roasting of nickel laterite, and (ii) reduction of basic nickel carbonate (BNC) and NiO to nickel. Nickel in laterite is associated with Fe-rich goethite and serpentine/olivine particles. Results indicate that the nickel recoveries from the limonite ores correspond closely to values predicted by thermodynamic modelling; nickel recoveries from serpentine ores are however significantly lower than these chemical equilibrium values. The nickel recovery from serpentine/olivine appears to be higher for particles with Mg to Fe mol ratio of lower than 8.

In relation to the reduction of BNC and NiO, the change of phase, product surface, internal microstructures taking place during reduction/oxidation of BNC at $110^{o}C$ to $900^{o}C$; as well as the kinetics and microstructure transformation mechanism during reduction of synthetic NiO at $400^{o}C$ to $1000^{o}C$ have been studied. A clear link has been established between the rates of reduction, the nickel product morphology, and the reaction mechanisms occurring at the Ni-NiO interface. A change in the reduction behaviour was observed between 600 and $800^{o}C$ depending on the hydrogen partial pressures and reduction time. The phenomena affecting the final-product microstructure were identified as follows: (1) chemical changes, i.e. decomposition, reduction and oxidation reactions; (2) NiO and Ni recrystallisation and grain growth; (3) NiO and Ni sintering and densification; and (4) agglomeration of the NiO and Ni particles.

1　Introduction

Nickel metal is widely used for many applications including for industrial, military, transport/aerospace, marine and architectural purposes because of its properties such as high resistance to corrosion and oxidation, excellent high-temperature strength and toughness, and relatively low thermal and electrical conductivities. Specifically, nickel is used mainly for manufacturing stainless

steel and non-ferrous alloys (including super-alloys). There has been an increasing trend in the demand of nickel for the past eight years [1]. This, in addition to the European Union's new environmental and chemical policy regulations [2] which require the nickel product to have oxygen concentration of less than 0.1 wt% as nickel oxide, has driven the improvement and optimisation of the current nickel production processes.

Nickel occurs in nature principally as sulphides and laterites (oxides and silicates). The principal source of primary nickel metal at present is sulphides; however, there is an increasing trend in using nickel laterite ores as the primary source as about 70% of world land based nickel resources are contained in laterites [3]. In general, nickel can be extracted from its ores using smelting, high pressure acid leaching (HPAL) and Caron roast/leach process [3, 4].

The current article discusses the fundamental studies carried out by the authors in support of improvement of nickel production process through Caron Process utilising nickel laterite as the primary source. Two major areas are described in this article: (1) reduction roasting of nickel laterite, and (ii) reduction of intermediate product of basic nickel carbonate (BNC) and NiO to nickel.
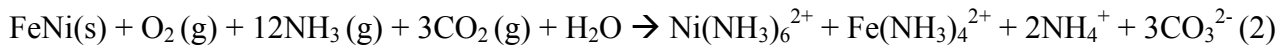
2   Caron Process

The Caron [5] process has been utilised for the production of nickel since 1944 and there are currently commercial operations at Nicaro, Punta-Gorda, and Yabulu/BHP-Billiton nickel [3]. In this article a modified-Caron process is described based on the operations at the BHP-Billiton Yabulu refinery [6]. In general the process consists of: ore beneficiation and blending, reduction roasting, leaching of roaster product in ammoniacal solvent, separation of Ni and Co using solvent extraction, precipitation from solution of basic nickel carbonate (BNC) intermediate product, and thermal decomposition of BNC to NiO and gaseous reduction of NiO to Ni.

The main feed for the process is a mixture of limonitic (Fe-rich oxides/hydroxides) and saprolitic (Mg-Fe silicates) nickel laterites. The mixture is dried to reduce moisture from 35% to approximately 8%. The dried laterites are then ground to size less than 850μm before they are fed into reduction-roasters.

The reduction-roasting is carried out in Herreshoff multiple hearth furnaces. Heavy fuel oil is mixed with the laterites to provide the high temperature inside the furnace through its partial combustion, and provide reducing agent for the reduction process. The maximum temperature of the reduction roasting process is 740-750°C. This process is the critical stage that determines the recovery of nickel from the laterite ores. The reduced ores discharged from the roasters and cooled under a neutral atmosphere to temperature below 250°C.

The cooled roaster product is subsequently leached in an ammonia-ammonium carbonate solution. In this process, the nickel is selectively leached from the solid. The simplified reactions of the leaching process are described as follows [7]:

$$Ni(s) + \tfrac{1}{2}O_2\,(g) + 8NH_3\,(g) + 2CO_2\,(g) + H_2O \rightarrow Ni(NH_3)_6^{2+} + 2NH_4^+ + 2CO_3^{2-} \qquad (1)$$

$$FeNi(s) + O_2\,(g) + 12NH_3\,(g) + 3CO_2\,(g) + H_2O \rightarrow Ni(NH_3)_6^{2+} + Fe(NH_3)_4^{2+} + 2NH_4^+ + 3CO_3^{2-}\ (2)$$

The pregnant liquor is then separated from the undissolved solid. Iron and cobalt are also dissolved into the ammonia-ammonium carbonate liquor. The Fe metal complex is unstable and reacts with the oxygen from the atmosphere and precipitates as solid iron hydroxide. Cobalt, on the other hand, is separated from the nickel by ammonium solvent extraction process and is extracted by hydro-metallurgical refining in a separate cobalt processing circuit [8]. The purified liquor is then steam stripped to remove ammonia-ammonium carbonate and to recover the nickel as basic nickel carbonate (BNC), i.e. a mixed carbonate hydroxide solid with approximately 52% nickel content (dry basis). The remaining liquid is separated from the solid by filtering process. The BNC has various compositions and is present in one of the following forms: $NiCO_3.xH_2O$, $NiCO_3.xNi(OH)_2.yH_2O$, $NiCO_3.xNiO.yH_2O$ [9].

The BNC is further processed through a series of high temperature processes involving various gas-solid reactions. The BNC at the Yabulu refinery is fed to a rotary kiln operated in slightly reducing atmosphere conditions, fired with naphta or coal seam gas. This process is aimed at partially reducing the BNC to Ni-NiO mixtures.

Dehydration and decomposition of BNC in the kiln occures through the following reactions [10]:

$$90\text{ - }200^{o}C:\quad xNiCO_3.yNi(OH)_2.zH_2O \rightarrow xNiCO_3.yNi(OH)_2 + zH_2O \qquad (3)$$

$$270\text{ - }420^{o}C:\quad xNiCO_3.yNi(OH)_2 \rightarrow (x+y)NiO + xCO_2 + yH_2O \qquad (4)$$

Partial reduction of nickel oxide takes place subsequent to the decomposition process:

$$NiO(s) + H_2/CO(g) \rightarrow Ni(s) + H_2O/CO_2(g) \qquad (5)$$

The kiln produces a mixture of metal-metal oxide containing 92% nickel. The second stage of the reduction process is carried out in a reduction furnace. The kiln product is crushed and mixed with saw dust to provide sufficient porosity in the bed during the reduction process. The residence time in the furnace is approximately one hour. The furnace carries out reduction at an average temperature of $900^{o}C$ under an atmosphere containing cracked ammonia, 75%H_2 and 25%N_2. The reduction furnace product contains approximately 97.5% Ni. The reduction furnace product is then crushed, blended with stearic acid and pressed into compacts. The compacts are then fed into sintering furnace, which has a similar operation as the reduction furnace. In the furnace, final stage of reduction and sintering of the nickel take place simultaneously. The final product of this process contains > 99% Ni.

3   Nickel Laterite Reduction Roasting

There has been a number of studies on the mineralogy and geochemistry of laterites, as well as reduction roasting and leaching of limonitic and saprolitic laterites [5, 11-14]. It is generally agreed that nickel is associated with either goethite or serpentine (lizardite) minerals which, during reduc-

tion roasting, are transformed to magnetite and olivine, respectively; as well as Ni-Fe alloy. Despite all of these studies, the mechanism of phase and microstructure transformations of the nickel bearing phases, especially serpentine are still not completely understood. Current research is centred on the investigation of the mechanisms of the nickel-bearing phase and microstructure transformations.
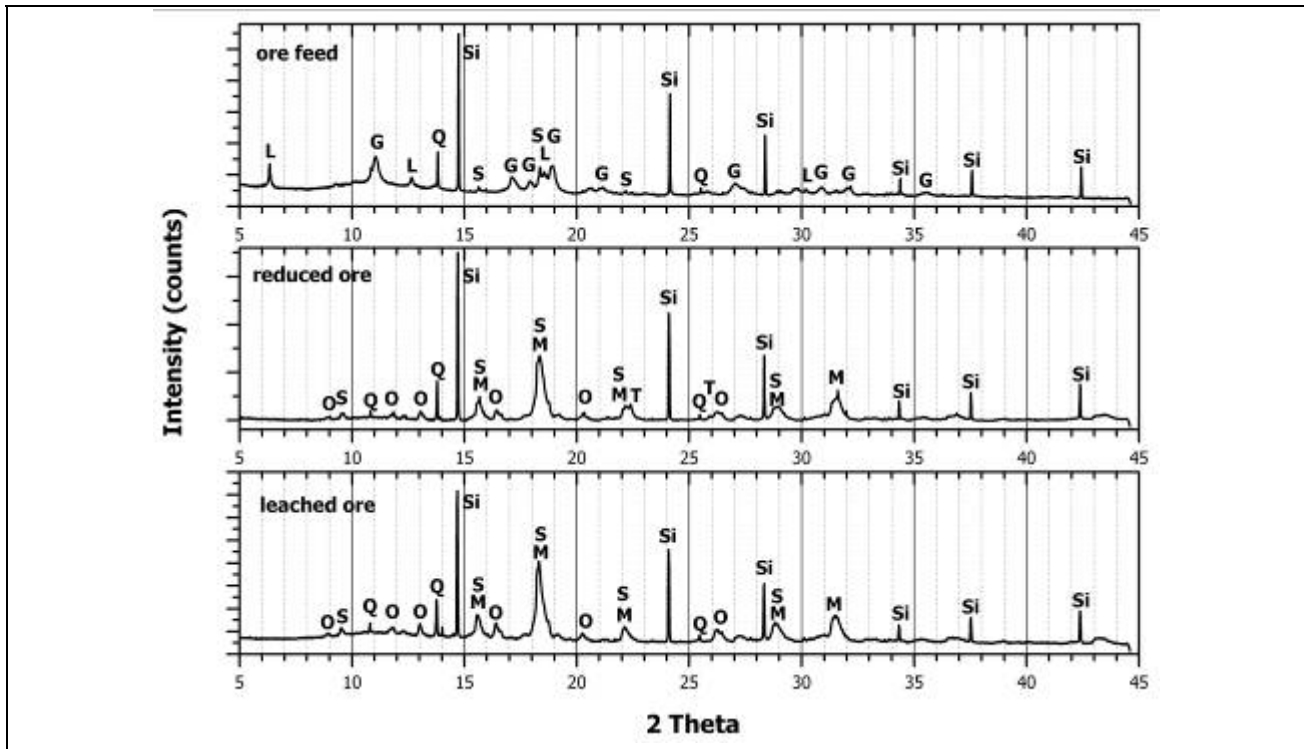

Figure 1:   Synchrotron XRD spectra (wavelength 0.8Å) of the initial, reduced and leached laterite ore samples. L = lizardite (serpentine), G = goethite, Q = quartz, Si = silicon standard, O = olivine, M = magnetite, S = spinel Fe-chromite, T = taenite (Fe-Ni alloy) [16]

Rhamdhani *et al.* [16] used electron probe microanalysis (EPMA) and synchrotron X-ray powder diffraction (SXRD) to study the detailed microstructural and phase changes in the limonitic-saprolitic ore mixtures during reduction roasting and leaching from the Yabulu process. The microstructures observed were quite complex and include composite, fine-grain mixture, intergrowth, vein-like/platelike, porous and dense microstructures. Figure 1 shows the SXRD results of the initial, reduced and leached ore samples from the nickel plant. In the initial ore mixture, the major phases identified include goethite $(Fe,Ni)O(OH)$, serpentine-lizardite $(Mg,Fe,Ni)_3Si_2O_5(OH)_4$, quartz SiO_2, and spinel Fe-chromite $(Fe,Mg)O\cdot(Cr, Al, Fe)_2O_3$. Upon reduction, olivine $(Mg,Fe,Ni)_2SiO_4$, magnetite $(Fe,Ni)O\cdot Fe_2O_3$, quartz, and spinel Fe-chromite were observed. In addition to these phases, taenite (Fe,Ni) alloy peaks were also observed in the spectra. These results are in agreement with previous studies on laterite reduction [14]. The SXRD spectrum observed in the leached ore was found to be similar to that from reduced ore, however, in the leached ore sample the peaks for taenite do not appear which suggests the metal (thus nickel) dissolution has taken place upon leaching.

From the EPMA analysis of the leached ores, Rhamdhani *et al.* [15] showed that most of the nickel was extracted from the limonite composite material. Conversely, significant residual nickel was observed in the olivine phase. Rhamdhani *et al.* [16] carried out thermodynamic modelling of limonitic and saprolitic laterite reduction roasting using FactSage thermodynamic package. The modelling results suggest that at the same conditions (i.e. oxygen partial pressure and temperature) the equilibrium nickel partitioning to the alloy for goethite matrix and serpentine/olivine is not the same, as shown in Figure 2(a). At $pO_2 = 10^{-19.5}$atm at 740^oC (i.e. the condition inside the hearth furnace, shown as shaded area in Figure 2), the fraction of nickel reporting to alloy in the case of goethite matrix is 0.92 (92%), while in the case of serpentine/olivine is only 0.58 (58%). The calculated equilibrium nickel recovery from the goethite matrix is in agreement with the actual nickel recovery measured using EPMA, i.e. 0.86 – 0.93 (86% – 93%). Importantly it shows that maximum nickel recovery from limonitic ores in this process can be predicted from phase equilibrium considerations.
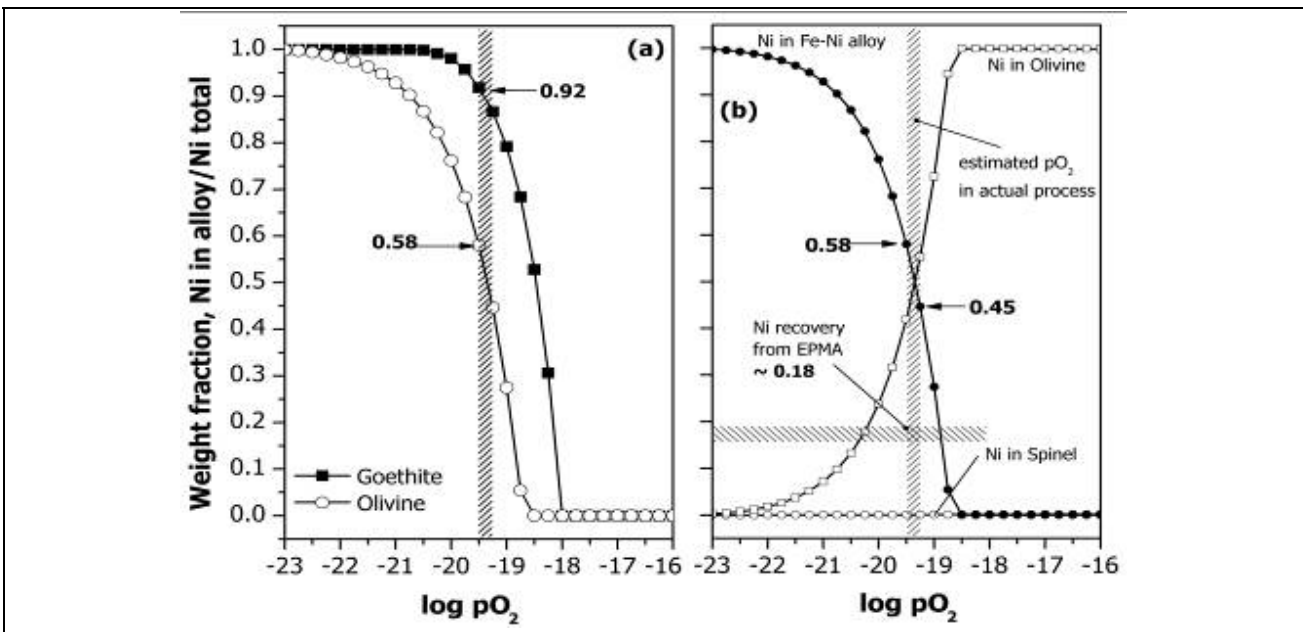

Figure 2:   Thermodynamic modelling using FactSage: (a) comparison of Ni partitioning to the alloy in the case of reduction roasting of goethite matrix and olivine; (b) equilibrium nickel distribution between alloy and olivine in the case reduction of olivine. T = 740^oC [16]

The equilibrium nickel distributions between olivine and Fe-Ni alloy are shown in Figure 2(b). The actual nickel recovery from the olivine phase measured using EPMA was 0.18 (18%); this is much lower than the calculated equilibrium values, i.e. between 0.45 - 0.58 (45% - 58%). These results indicate that the optimum conditions for reduction roasting of the two types of laterite (limonitic and saprolitic) are different and should be taken into account when mixtures of the two types of laterites are used as feed for the process.

The information on the mechanism of phase transformation of the phases, especially serpentine and goethite, during reduction roasting process is important for improvement of the overall nickel yield from the ores. Formation of Ni-Fe alloy after reduction roasting, which is then leached out in the

subsequent leaching process has been suggested in the previous studies [14], however, to date there has not been any direct evidence showing the formation of these particles, e.g. detailed morphology and size. Rhamdhani *et al.* [16] using high resolution scanning electron microscope (HRSEM) observed submicron (15-20nm) metallic particles which appears to be Fe-Ni alloy particles formed at the free surfaces and interspersed within the porous magnetite. However, these particles were not observed in the olivine particles. This probably due to the fact that the optimum conditions between the two types of ores are different, as suggested in Figure 2.
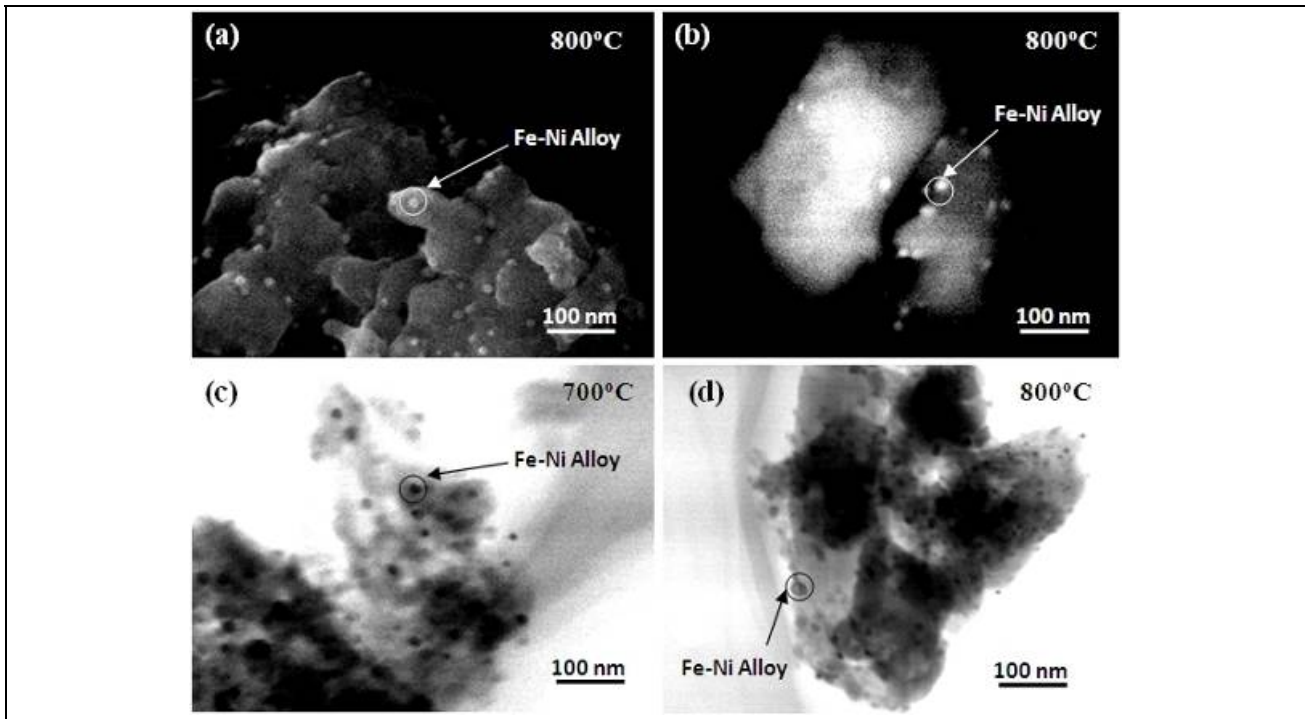

Figure 3:   (a) HRSEM secondary electron imaging, (b) HRSEM backscattered electron imaging, (c) and (d) TEM imaging (bright field, STEM mode) of serpentine reduced in 15%H_2-N_2 for 30 min at 700°C and 800°C [17].

Chen *et al.* [17] conducted laboratory studies on the reduction roasting of separate serpentine particles in 15%H_2-N_2 atmosphere, which is a more reducing condition compared to the condition inside the industrial hearth furnaces. In this study, both high resolution scanning electron microscopy (HRSEM) and transmission electron microscope (TEM) were used to analyse the reduced and leached ore samples. Chen *et al.* [17] observed the formation of nano-particles on olivine particles upon reduction.

Figures 3(a) and 3(b) show HRSEM secondary and backscattered electron images of reduced saprolite ore in 15%H_2-N_2 for 30 minutes at 800°C, showing precipitates with particle size about 10-20 nm forming on the surface of the olivine. TEM imaging, Figures 3(c) and 3(d), with combined energy dispersive x-ray (EDX) analysis, Figure 4(a), show high content of nickel and iron in these precipitates. These precipitates were not observed in the original serpentine particles, indicating that the Ni-Fe alloy precipitate was formed due to the reduction process. The selected area diffraction pattern of the alloy precipitates suggests a face centred cubic structure, as shown in Figure 4(b).

Chen *et al.* [17] observed that surface precipitates were formed after reduction at 700°C and 800°C and the size was found to increase with increasing of reduction temperature. These micrographs represent first direct observations of Ni-Fe alloy precipitates formed during the reduction roasting of laterite ores.

Chen *et al.* [17] also conducted leaching of the reduced serpentine ores and found that nickel recovery increases with increasing reduction temperature up to 750°C. At 800°C, however, the nickel recovery was decreased significantly. Stevens *et al.* [18] suggested that re-dissolution of the nickel in the olivine phase at higher temperature results in this lower nickel recovery. However, as can be seen from Figures 3(d) and 4(a), that at 800°C, a large amount of Ni-Fe alloy precipitates were formed and showed no sign of re-dissolution to olivine phase.

Upon leaching, Chen *et al.* [17] observed that while the Ni-Fe alloy precipitates on the surface of the olivine particles were removed, significant amounts of such precipitates remained in the interior of the particles. Morphological studies of serpentine during reduction roasting indicate the formation of pores, coarsening of pores and closing up of pores as the serpentine was reduced at higher temperature. Therefore, it appears that the mechanism of the lowering of nickel recovery at higher temperature reduction is due to the physical entrapment of the Ni-Fe alloy nano-precipitates resulting in inacessibilty of leaching liquor.

Rhamdhani *et al.* [15] attempted to correlate the chemistry of the olivine (reduced and leached in industrial processes) with its nickel recovery. Figure 5 shows the plot of nickel concentrations *vs* the Mg to Fe mol ratio in the olivine particles measured using EPMA. The open triangles and the closed circles are the actual nickel concentration for the reduced and the leached olivines obtained from industrial processes, respectively. The differences in metal concentrations between these may indicate the extent of nickel recovery upon leaching. In general it can be seen from Figure 5 that the olivines with Mg to Fe ratios lower than 8 appear on average to produce better nickel recoveries compared to olivine with Mg to Fe ratios higher than 8. This trend may be attributed to the alteration stage of the initial serpentine ore (i.e. from stage 1 to 5 as shown by the dashed lines in Figure 5), which govern the physical characteristics of the ore, such as detailed microstructure (dense, vein-like), porosity and crystallinity. The alteration stage of the initial ore reflects to its chemical composition, i.e. to its Mg to Fe ratios. The trend may also be attributed to the thermodynamic characteristic of the olivine, in particular the activity of NiO in the olivine. The activity of NiO is affected by the composition of the olivine, thus also affected by the Mg to Fe ratio in the olivine.
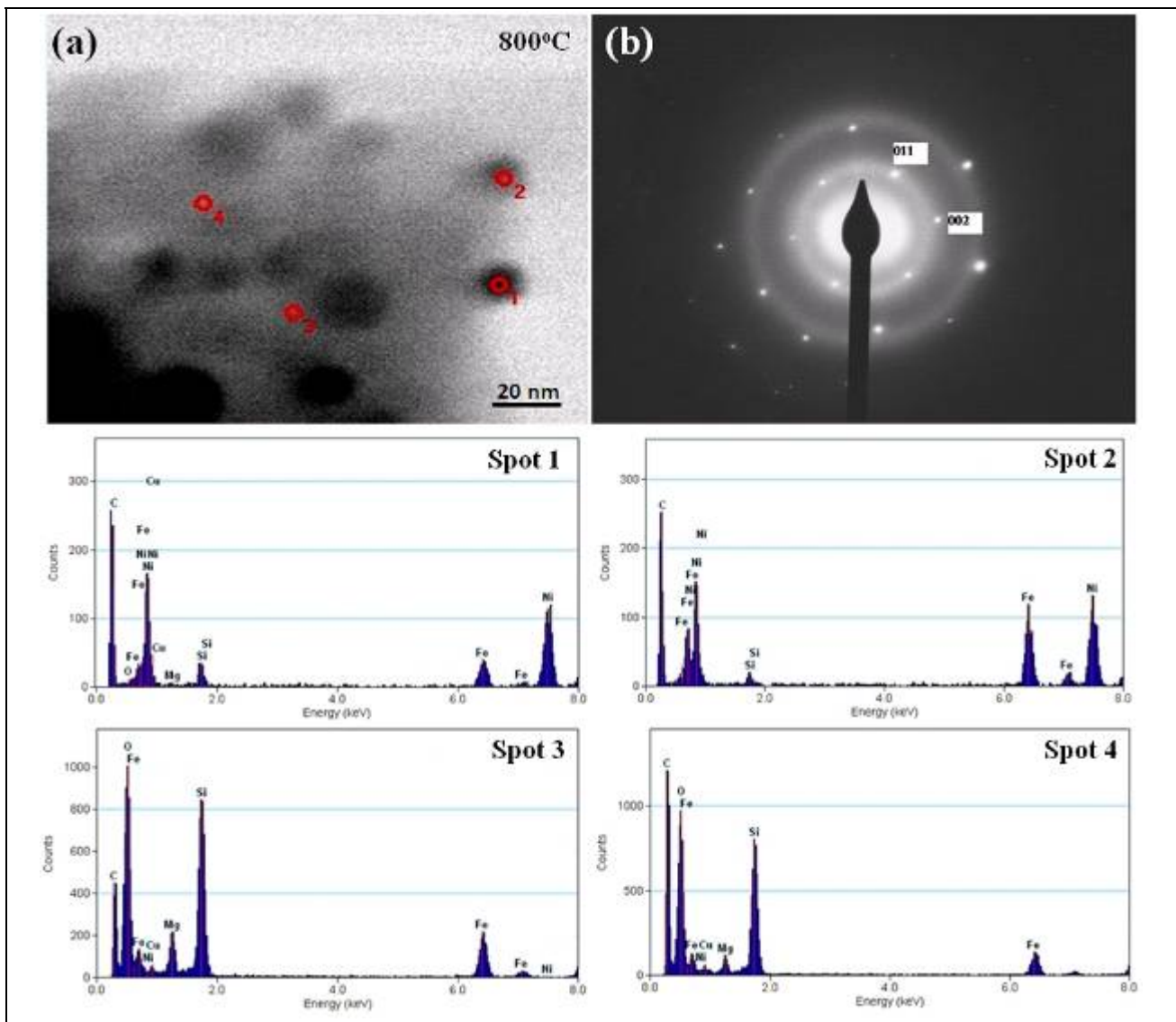
Figure 4: (a) TEM image of reduced serpentine showing spots showing energy dispersive X-ray (EDX) analyses of the Ni-Fe precipitates (Spots 1 and 2) and olivine matrix (Spots 3 and 4). (b) selected area diffraction (SAD) pattern of the alloy precipitate. [17]

As can be seen from the above that the factors affecting the overall nickel recovery from olivine particle are quite complex; it is affected by: (1) the physical characteristics of the particles, e.g. particle size, detailed microstructure (dense, vein-like), porosity and crystallinity; (2) the thermal history of the materials (e.g. reduction roasting); (3) the details of leaching practice; and (4) its chemical characteristics, such as Mg to Fe ratio, i.e. the degree of solid solution between fayalite (Fe_2SiO_4) and forsterite (Mg_2SiO_4). Currently, work is underway at the Pyrometallurgy Research Centre, University of Queensland, to develop a more complete understanding of the detail mechanisms of the serpentine phase and microstructure transformation upon reduction roasting and leaching processes.
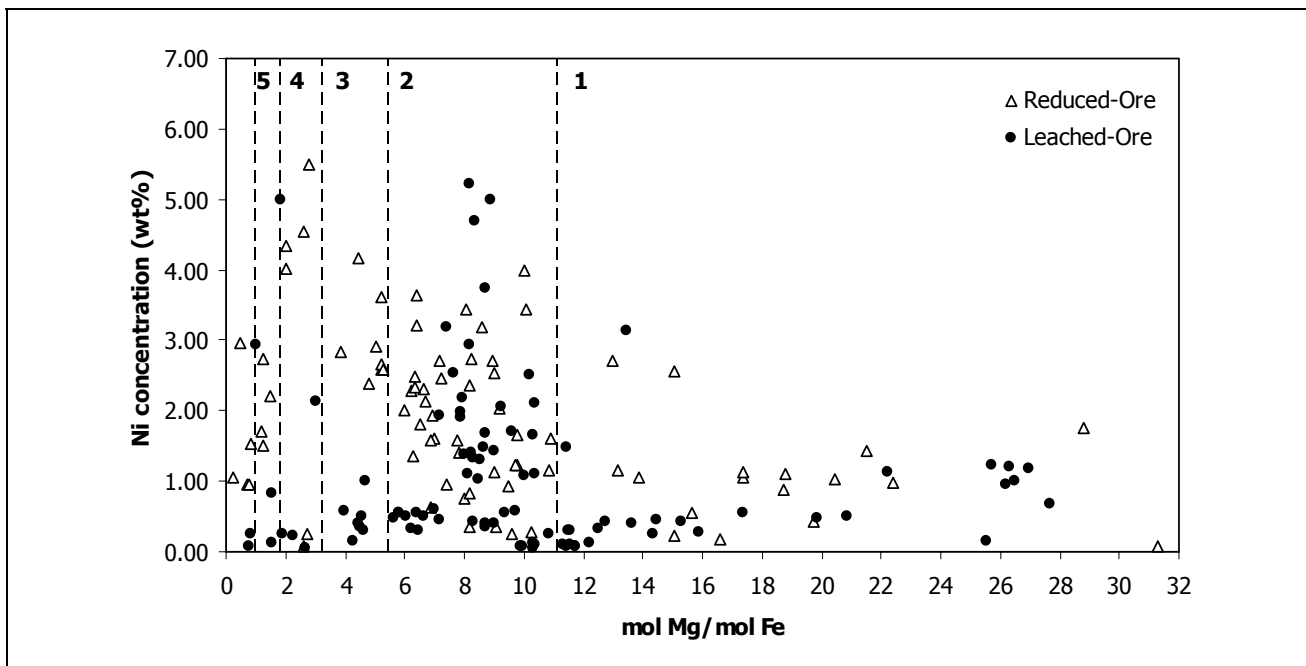
Figure 5: Nickel concentration (in wt %) *vs* Mg to Fe ratio in the olivine phases of the reduced ore (open triangles) and leached ore (closed circles) samples from industrial process.

4 Basic Nickel Carbonate (BNC) and Nickel Oxide Reduction

The reduction of the BNC to NiO and subsequently to Ni involves various fundamental phenomena that may occur simultaneously during processing. These may include (but are not limited to) solid decomposition, reduction and oxidation reactions, gas and solid phase mass transfers, nucleation and growth, and sintering. Understanding the detail of the fundamental mechanism of the process is vital for the development of process strategies in industry for achieving very low oxygen concentration in the final product.

Rhamdhani *et. al.* [10] analysed and classified the microstructures of the residual NiO observed in the samples obtained from several locations along the process lines in industrial production of Ni in the Yabulu refinery. The types of NiO observed, as can be seen in Figure 6, include: (a) Type 1 - Trapped round particles surrounded by: (1A) thick or (1B) thin dense Ni; (b) Type 2 - Trapped blocky form surrounded by porous Ni; (c) Type 3 - Surface layer of a NiO on Ni particle: (3A) with or (3B) without a fine layer of Ni on oxide surface; (d) Type 4 - Bulky NiO: (4A) with or (4B) without dense Ni inside; and (e) Type 5 - Fine partially reduced NiO particles with individual particle size of 1 to 5μm. These microstructures are produced by the various combinations of fundamental reactions occurring during the industrial process. Of the above, Type 1A is the most undesirable; it is very difficult to remove residual oxygen as there is no reducing gas access to the NiO in the interior of the particle, and further reduction of NiO can only occur by solid state diffusion of oxygen through the dense nickel layer.
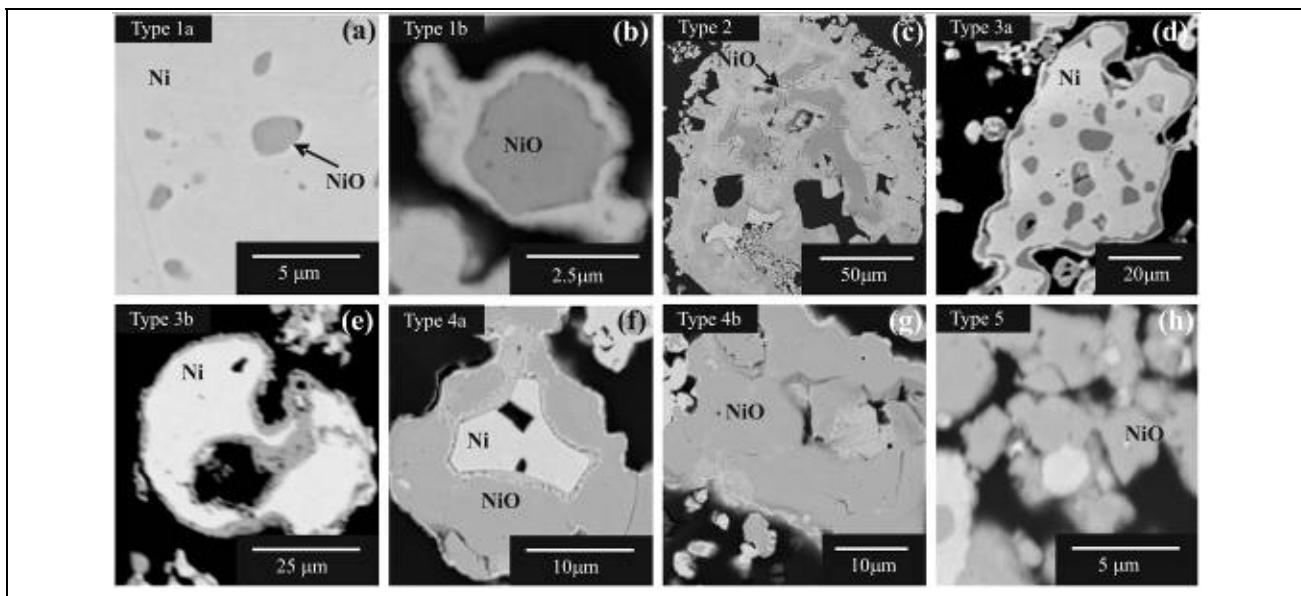
Figure 6:   Examples of types of residual NiO observed in the materials and product of refinery plant: (a) Type 1A, (b) Type 1B, (c) Type 2, (d) Type 3A, (e) Type 3B, (f) Type 4A, (g) Type 4B, and (h) Type 5. [10]

Following careful evaluation of the modes of occurrences of residual NiO in the materials, the thermal and atmosphere conditions in the industrial process; and consideration of possible elementary reactions and phenomena involved in the gas-solid reaction processes; Rhamdhani *et. al.* [10] then conducted a systematic laboratory study on the oxidation and reduction reaction of BNC. Single and multiple-stage non-isothermal heat treatments were carried out on BNC samples at temperatures 110°C to 900°C under specifically designed conditions to reproduce some of the residual NiO microstructures observed in plant practice to enable the underlying elementary reactions and fundamental phenomena occurring during the process responsible for the formation of these microstructures to be investigated. The heat treatments carried out include: (1) calcination of BNC in air, (2) direct reduction of BNC in 15%H_2-N_2 and 1.5%H_2-N_2 atmospheres, and (3) reduction in 15%H_2-N_2 gas atmosphere of pre-calcined BNC. A heating rate of 10°C/min used in the study was selected to reflect the heating rate in the rotary kiln used in industrial production of nickel at Yabulu.

It was found [10] that both in the oxidising and reducing conditions, upon increasing the temperature, BNC decompose in two stages. The first stage involve the removal of physically absorbed water (at 90°C to 200°C), while on the second stage BNC decomposes to NiO accompanied by the removal of chemically bound H_2O and CO_2 (at 270°C to 420°C).

In the case of oxidising condition (in air), at 660°C to 700°C, the recrystallisation of NiO commenced; as the temperature increased, sintering and grain growth of the recrystallised NiO grains took place within the original particles. By 700°C, these processes have resulted in a significant decrease of specific surface area, and at 900°C, fully recrystallised NiO particles were formed, as shown in Figure 7(a).

In the case of reduction in 15%H_2-N_2, once the NiO was crystallised at about 340°C, nucleation and growth of Ni was found from XRD and microscopy examination to occur under these conditions. At temperatures between 600°C to 800°C, sintering and agglomeration of the nickel product takes place. At 900°C, 0.5 to 10μm dense Ni grains were observed with no evidence of residual NiO, as shown in Figure 7(b).

When the BNC was pre-oxidised/pre-calcined to 900°C prior to reduction, residual NiO (Type 1A) in the nickel product was observed, as shown in Figures 7(c) and 7(d). It was suggested that this was due to a slower NiO reduction rate due to larger grain size, denser sintered structure and higher crystallinity (lower reducibility) of the recrystallised NiO as a result of pre-oxidation at 900°C. However, when the pre-oxidation was carried at temperatures below recrystallisation temperature of NiO (e.g. at 700°C and 500°C), the residual NiO was not observed after subsequent reduction, as shown in Figures 7(e) and 7(f), respectively.

Rhamdhani *et al.* [10] also found that when the partial pressure of hydrogen was decreased by one order of magnitude, i.e. from 15%H_2-N_2 to 1.5%H_2-N_2 (decreasing the kinetics of reduction), residual NiO enclosed by dense nickel layer was observed at 900°C, as shown in Figure 7(g). In this case the overall rate of NiO reduction was in general slower than the rate of densification of the nickel product. As a result, the nickel product at the surface formed a dense low permeability layer and enclosed the unreduced NiO. Residual NiO, once formed in this Type 1A morphology is difficult to remove.
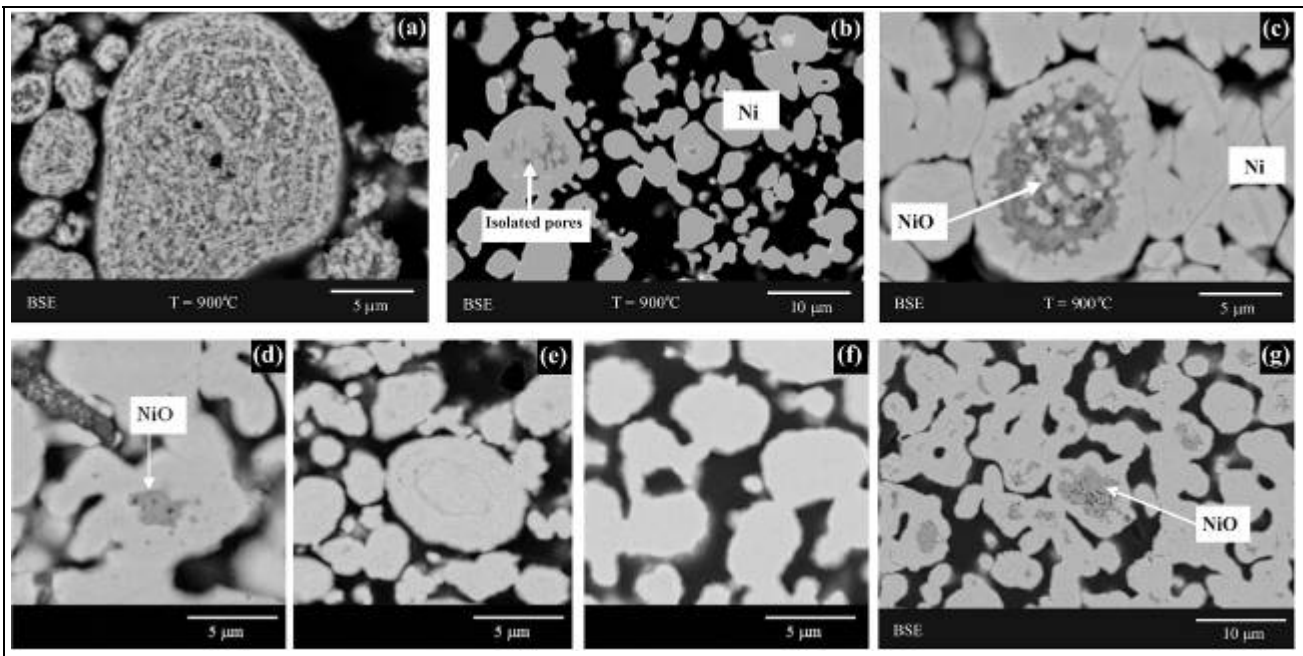

Figure 7:　Backscattered electron images of BNC particles section: (a) calcined in air at 900°C and (b) reduced in 15%H_2-N_2 at 900°C; pre-calcined in air at (c) and (d) 900°C, (e) 700°C, (f) 500°C then reduced in 15%H_2-N_2 at 900°C; and (g) reduced in 1.5%H_2-N_2 at 900°C. All used 10°C/min heating rate and holding time 30 minutes. [10]

A separate study [20] has been carried out to investigate the various interfacial microstructures formed during partial reduction of dense synthetic NiO strip in H_2/N_2 and H_2/H_2O atmospheres at temperatures 300°C to 1000°C. Four types of structures were observed, namely: (1) coarse fibrous nickel with fissures, (2) fine porous nickel with planar interface, (3) large porous nickel with irregular interface and (4) dense nickel layer; as shown in Figure 8.

These microstructures formed depending on the reduction conditions, reaction temperature, hydrogen partial pressure and H_2/H_2O ratio. Maps of the interfacial microstructure as a function of temperature, H_2 partial pressure, and thermodynamic driving force of reduction (H_2/H_2O ratio) are described in detail by Hidayat *et al.* [21] in another study. In general, the transition from the coarse fibrous nickel with fissures towards the fine porous nickel-planar interface and large porous nickel-irregular interface structures is promoted by the increase of temperature and the decrease of hydrogen partial pressure. Furthermore, high concentrations of steam content (low thermodynamic driving force) in the reducing gas results in the formation of dense nickel layer. The general mechanism of the formation of these micrsotructures have been described by Hayes [22].
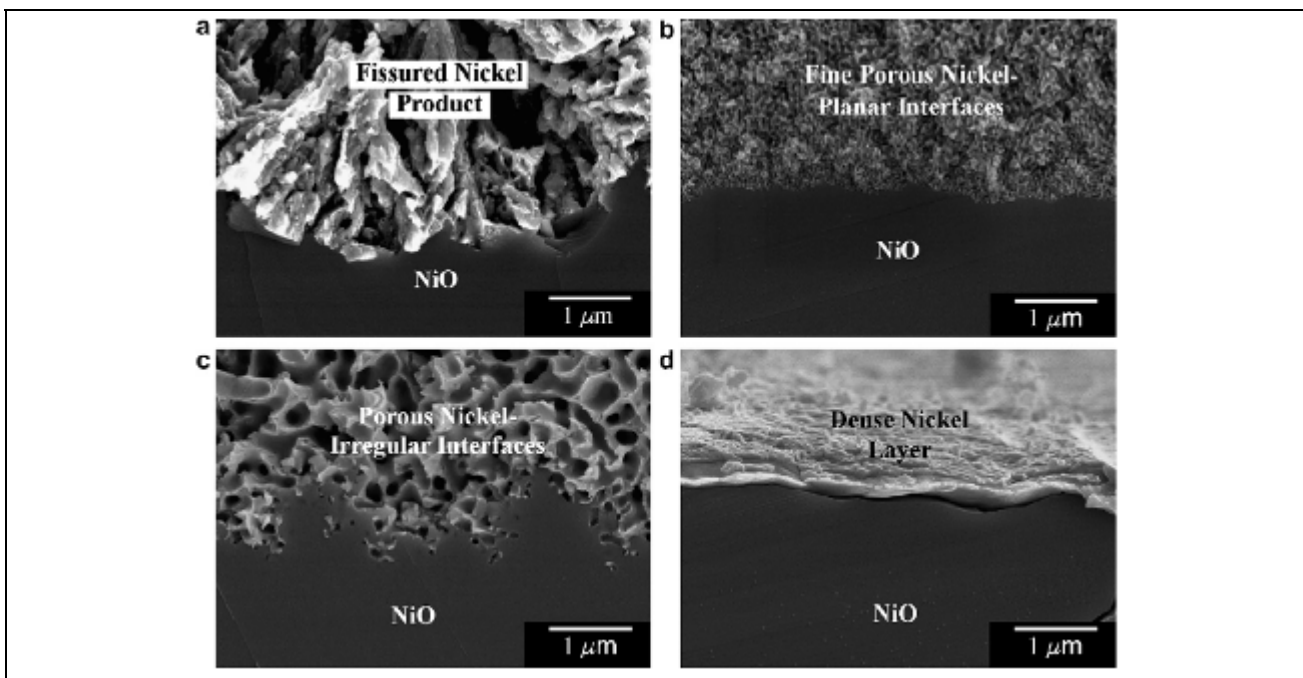

Figure 8:   Interfacial structures formed during the reduction of dense synthetic NiO: (a) 300°C-100% H_2-300s, (b) 500°C-100% H_2-10s, (c) 800°C-100% H_2-10s (d) 1000°C-2% H_2 and 98% H_2O-320s. [20]

Rhamdhani *et al.* [10, 19] indicated that on reduction of BNC at temperature range between 700°C and 800°C various processes that can affect the extent of oxygen removal occur simultaneously, these include recrystallisation, grain growth, densification and agglomeration of nickel particles. At the same temperature range, a slowdown in the rate of NiO reduction at this temperature range was also observed [23, 24], as shown in Figure 9. Hidayat *et al.* [27] correlated the interface microstructures and the kinetics information on the reduction of NiO. It has been suggested that a transition

from a continuous cooperative growth mechanism, in which simultaneous chemical reaction and mass transport processes occur, to a discontinuous process involving pore growth, coverage of pores by metal, bursting of metal layers and the repeated cycle of these latter process steps to be most likely explanation for the observed slowdown.
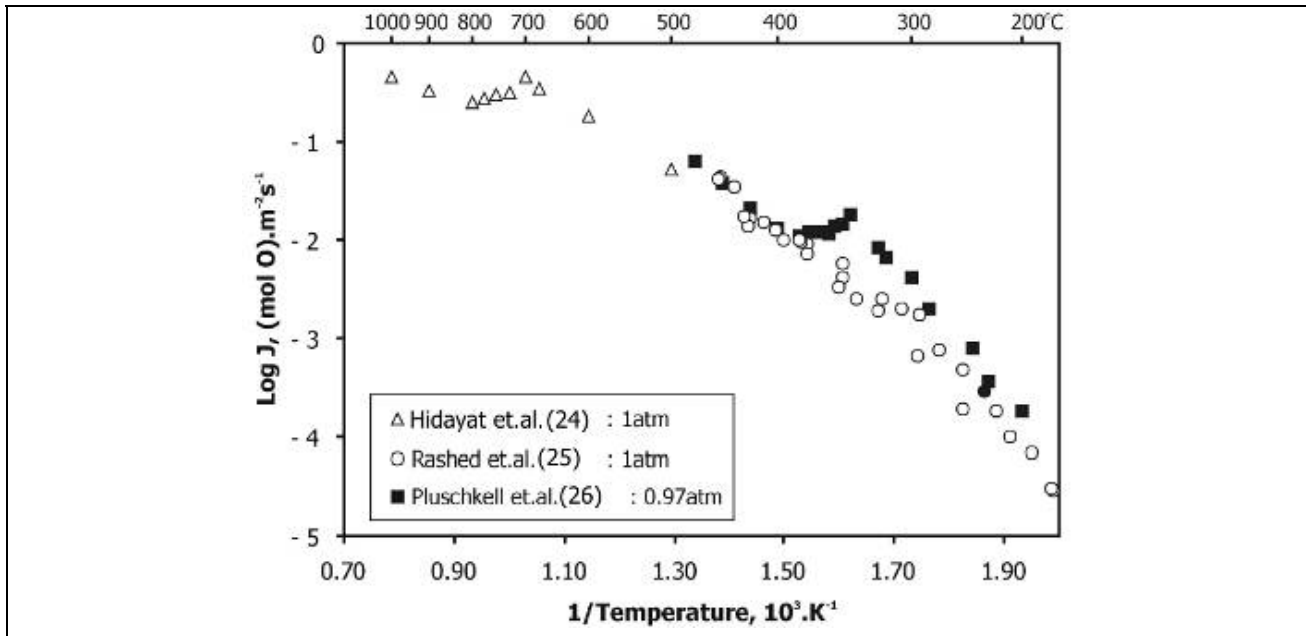

Figure 9:   Arrhenius plot of initial reaction rate of NiO reduction (in terms of flux of oxygen removal) from Hidayat *et al.* [24], Rashed *et al.* [25] and Pluschkell and Sarma [26].

The results presented clearly show that the material's thermal history and original microstructure have significant effects on the microstructure evolution, hence on the final microstructure of the nickel product. The fundamental phenomena that are observed to contribute to the change of the physical and chemical characteristics of the particles during the process, affecting the final microstructure, include: (1) Chemical changes, i.e. decomposition, reduction reaction, oxidation reaction; (2) NiO and Ni re-crystallisation and grain growth; and (3) NiO and Ni sintering and densification. These findings have clear implications for industrial practice, demonstrating that the key to achieve complete reduction of NiO by hydrogen gas is by control of the relative rates of densification of nickel product and the overall reduction rate of nickel oxide. The high extent of NiO reduction is favoured by: (1) maintaining a high NiO specific surface area, avoiding NiO and Ni recrystallisation and densification; and by (2) utilise high chemical driving force for reduction, which is favoured by high H_2 partial pressures and high H_2/H_2O ratios.

5   Conclusions

Recent research in support of the improvement of nickel production through the Caron process, focused on the improvement of reduction roasting process and reduction of BNC and NiO, has been described in the present article.

It has been shown by thermodynamic calculations that the optimum conditions for the reduction roasting of limonitic and saprolitic laterites are different. The recovery of nickel from the limonite ores closely approximates the values predicted assuming chemical equilibrium is achieved during the reduction roast process. The factors affecting the overall nickel recovery from the ores are quite complex; it is affected by the physical and chemical characteristics of the particles, the thermal history of the materials, and the details of leaching practice.

It has also been shown that the material's thermal history and original microstructure have significant effects on the microstructure evolution, hence on the final microstructure of the nickel product. The fundamental phenomena that contribute to the change of the physical and chemical characteristics of the particles during the process, affecting the final microstructure were also identified. It has been demonstrated that the key to achieve complete reduction of NiO by hydrogen gas is by control of the relative rates of densification of nickel product and the overall reduction rate of nickel oxide.

6   Acknowledgements

7   References

[1]   INSG – INTERNATIONAL NICKEL STUDY GROUP: World statistic data on nickel production and usage. 23 October 2008, http://www.insg.org/stats.aspx (accessed 20 Nov 2008).

[2]   BERGESON, L.L.: EU's new chemical policy will hurt competitiveness. Chemical Processing. 9 October 2003, http://www.chemicalprocessing.com/articles/2003/143.html?page=print (accessed 20 Nov 2008).

[3]   DALVI, A.D., BACON, W.G. and OSBORNE, R.C.: The past and the future of nickel laterites. PDAC 2004 International Convention Trade Show and Investors Exchange., Toronto, Canada, 7-10 March 2004, pp. 1-27.

[4]   BERGMAN, R.A.: Nickel production from low-iron laterite ores: process descriptions. CIM Bulletin. 96 (2003), pp. 127-138.

[5]   CARON, M.H.: Fundamental and practical factors in ammonia leaching of nickel and cobalt ores. Journal of Metals. 188 (1950), pp. 67-90.

[6]   FITTOCK, J.E.: Nickel and cobalt refining at QNI Pty Ltd Yabulu Queensland. AUSIMM Monograph 19, 2nd Ed. (1992), pp. 1-47.

[7]   NIKOLOSKI, A.N.: The electrochemistry of the leaching of pre-reduced Ni-laterites in ammonia-ammonium carbonate solution. PhD Thesis, Murdoch University, Australia (2002).

[8]   REID, J.G. and FITTOCK, J.E.: Yabulu 25 years on. International Laterite Nickel Symposium. The Minerals, Metals and Materials Society, Charlotte, NC, USA, (2004), pp. 599-618.

[9]   CANTERFORD, J.H.: Treatment of nickeliferous laterites. Minerals Science and Engineering. 7 (1975), pp. 3-17.

[10] RHAMDHANI, M.A., JAK, E. and HAYES, P.C.: BNC. Part I Microstructure and phase changes during oxidation and reduction processes. Metallurgical and Materials Transactions B. 39B (2008), pp. 218-233.

[11] CHEN, T.T., DUTRIZAC, J.E., KRAUSE, E. and OSBORNE, R.: Mineralogical characterization of nickel laterite from New Caledonia and Indonesia. International Laterite Nickel Symposium. The Minerals, Metals and Materials Society, Charlotte, NC, USA, (2004), pp. 79-99.

[12] DE GRAAF, J.E.: Treatment of lateritic Ni ores. Part I. Hydrometallurgy. 5 (1979), pp.47-65.

[13] DE GRAAF, J.E.: Treatment of lateritic Ni ores. Part II. Hydrometallurgy. 5 (1980), pp.255-271.

[14] VALIX, M. and CHEUNG, W.H.: Study of phase transformation of laterite ores at high temperature. Minerals Engineering. 15 (2002), pp. 607-612.

[15] RHAMDHANI, M.A, HAYES, P.C. and JAK, E.: Ni-laterites. Part I. Microstructure and phase characterisation. Mineral Processing and Extractive Metallurgy (Sec. C. Trans. IMM), (2008).

[16] RHAMDHANI, M.A, HAYES, P.C. and JAK, E.: Ni-laterites. Part II. Thermodynamic analysis of phase transformations. Mineral Processing and Extractive Metallurgy (Sec. C. Trans. IMM), (2008).

[17] CHEN, J., RHAMDHANI, M.A, HAYES, P.C. and JAK, E.: Unpublished work, Pyrometallurgy Research Centre, University of Queensland, Brisbane, Australia (2008).

[18] STEVENS, L.G., GOELLER, L.A. and MILLER, M.: The UOP nickel extraction process – An improvement in the extraction of nickel from laterites. Canadian Institute of Mining and Metallurgy, 14th Annual Conference of Metallurgists, Edmonton, Alberta, Canada (1975).

[19] RHAMDHANI, M.A., JAK, E. and HAYES, P.C.: BNC. Part II Microstructure evolution during industrial nickel production from basic nickel carbonate. Metallurgical and Materials Transactions B. 39B (2008), pp. 234-245.

[20] HIDAYAT, T., RHAMDHANI, M.A., JAK, E. and HAYES, P.C.: The characterization of nickel metal pore structures and the measurement of intrinsic reaction rate during reduction of nickel oxide in H_2-N_2 and H_2-H_2O atmospheres. Minerals Engineering. 21, (2008), pp. 157-166.

[21] HIDAYAT, T., RHAMDHANI, M.A., JAK, E. and HAYES, P.C.: The investigation of nickel product structures developed during gaseous reduction of solid NiO. Metallurgical and Materials Transactions B. Submitted 26 Aug 2008, (2008).

[22] HAYES, P.C.: A review of the mechanisms of decomposition of solids and their relevance to extractive metallurgical processes. Minerals Processing and Extractive Metallurgy Review. 8, (1992), pp. 73-94.

[23] UTIGARD, T.A., WU, M., PLASCENCIA, G. and MARIN, T.: Reduction kinetics of Goro nickel oxide using hydrogen. Chemical Engineering Science. 60 (7), (2005), pp. 2061-2068.

[24] HIDAYAT, T., RHAMDHANI, M.A., JAK, E. and HAYES, P.C.: The kinetics of reduction of dense synthetic NiO in H_2/N_2 and H_2/H_2O atmospheres. Metallurgical and Materials Transactions B. Accepted November 2008, (2008).

[25] RASHED, A.H. and RAO, Y.K.: Kinetics of reduction of nickel oxide with hydrogen gas in the $230 - 452^{\circ}C$ range. Chemical Engineering Communication. 156, (1996), pp. 1-30.

[26] PLUSCHKEL, W. and SHARMA, B.V.C.: Growth of cobalt and nickel during reduction of cobaltous and nickelous oxide with hydrogen. Arch. Eisenhuttenwes. 45, (1974), pp. 23-31.

[27] HIDAYAT, T., RHAMDHANI, M.A., JAK, E. and HAYES, P.C.: On the relationships between the kinetics and mechanisms of the gaseous hydrogen reduction of solid nickel oxide. Metallurgical and Materials Transactions B. Submitted 30 August 2008, (2008).